



Identification of serum biomarkers of chemoradiosensitivity in esophageal cancer via the targeted metabolomics approach

Fujigaki, Seiji ; Nishiumi, Shin ; Kobayash, Takashi ; Suzuki, Makoto ; Iemoto, Takao ; Kojima, Takashi ; Ito, Yoshinori ; Daiko, Hiroyuki ;...

(Citation)

Biomarkers in Medicine, 12(8):827-840

(Issue Date)

2018-08

(Resource Type)

journal article

(Version)

Accepted Manuscript

(Rights)

© 2018 Future Medicine Ltd

(URL)

<https://hdl.handle.net/20.500.14094/90007061>



Abstract

Aim: To identify the serum metabolomics signature that is correlated with the chemoradiosensitivity of esophageal squamous cell carcinoma (ESCC).

Materials & Methods: Untargeted and targeted metabolomics analysis of serum samples from 26 ESCC patients, which were collected before the neoadjuvant chemoradiotherapy, were performed.

Results: On receiving the results of untargeted metabolomics analysis, we performed the targeted metabolomics analysis of the 6 metabolites (arabitol, betaine, glycine, L-serine, L-arginine, and L-aspartate). The serum levels of the 4 metabolites (arabitol, glycine, L-serine, and L-arginine) were significantly lower in the patients who achieved pathological complete response with neoadjuvant chemoradiotherapy compared with the patients who did not achieve pathological complete response ($p=0.0086$, 0.0345 , 0.0106 , and 0.0373 , respectively).

Conclusion: The serum levels of metabolites might be useful for predicting the chemoradiosensitivity of ESCC patients.

Keywords: Esophageal squamous cell carcinoma, Metabolomics, targeted metabolomics analysis,

Predictive biomarkers, Chemoradiosensitivity, neoadjuvant therapy, 5-fluorouracil, Cisplatin

Introduction

Esophageal cancer is the sixth-leading cause of cancer death worldwide, and there were 400,000 deaths from esophageal cancer in 2012¹. Surgical resection is a reliable treatment for esophageal cancer, but a large number of patients develop locoregional recurrence and/or distant metastasis in the early period after surgery, and the prognosis of these patients is poor (median post-recurrence survival: 3 to 10 months)². To improve tumor resectability and survival in patients with locally advanced esophageal cancer, various trials of neoadjuvant chemotherapy or chemoradiotherapy followed by surgery have been attempted³⁻⁶. Some clinical trials and meta-analyses have suggested that neoadjuvant chemoradiotherapy plus surgery improves the overall survival of patients with potentially curable esophageal cancer⁵⁻⁷. However, neoadjuvant chemoradiotherapy does not have beneficial effects in all patients. Given that it is associated with various adverse effects and delays surgery, neoadjuvant chemoradiotherapy is harmful to non-responders; i.e., the prognoses of non-responders to neoadjuvant chemoradiotherapy were found to be

worse than those of responders⁸⁻¹⁰. Furthermore, non-responders exhibited worse outcomes than patients that underwent primary resection¹¹. Therefore, reliable methods for predicting the response of esophageal cancer to chemoradiotherapy are desired.

Cancer is currently regarded to be a metabolic disease¹². Metabolomics, which is a promising field of system biology, aims to investigate the sets of metabolites present in biological systems. Alterations in the levels of metabolites are influenced by changes in gene or protein expression, and hence, are closely related to actual phenotypes^{13,14}. Therefore, metabolomics has been used for research into biomarkers of many human diseases¹⁴⁻¹⁷, and we have also employed metabolomics in studies of various human diseases, including cancer¹⁸⁻²³.

In this study, untargeted metabolomics analysis based on gas chromatography/mass spectrometry (GC/MS) and liquid chromatography/mass spectrometry (LC/MS) of serum samples from esophageal cancer patients who received neoadjuvant chemoradiotherapy followed by surgical resection was performed to identify biomarker candidates for predicting the response of esophageal cancer to chemoradiotherapy. Then, we performed a targeted metabolomics analysis to quantify the serum levels of predictive biomarker candidates that were identified during the untargeted metabolomics analysis. The quantitative analysis revealed that the serum levels of 4 metabolites were

correlated with the response of esophageal cancer to neoadjuvant chemoradiotherapy, and moreover, showed that the serum L-serine level have a possibility of predicting the outcomes of esophageal cancer patients.

Materials and Methods

Patients and serum samples

Serum samples from 26 stage II-III (excluding T4) esophageal squamous cell carcinoma (ESCC) patients who were enrolled in a phase II clinical trial of neoadjuvant chemoradiotherapy conducted at the National Cancer Center Hospital (Tokyo, Japan) and National Cancer Center Hospital East (Chiba, Japan) between 2010 and 2011 were analyzed²⁴. The ESCC were pathologically diagnosed via pretreatment endoscopic biopsy examinations and clinically staged according to the Union for International Cancer Control TNM cancer staging system (the 6th and 7th editions). The neoadjuvant chemoradiotherapy consisted of two courses of a protracted 5-fluorouracil (5-FU) infusion (1,000 mg/m²/day, days 1-4) and a 2-hr cisplatin (CDDP) infusion (75 mg/m², day 1), with a 4-week interval between the courses, and concurrent radiotherapy (1.8 Gy/day, total radiation dose: 41.4 Gy). Transthoracic esophagectomy combined with extensive lymphadenectomy (>D2) was

performed at 6 to 8 weeks after the completion of the chemoradiotherapy. The effects of the neoadjuvant chemoradiotherapy were evaluated by both clinical response and pathological response according to the 10th edition of the Japanese Classification of Esophageal Cancer. The pathological responses were evaluated in the surgical specimens and then were classified into grade 0 (ineffective), grade 1 (slightly effective), grade 2 (moderately effective), and grade 3 (markedly effective). The pathological responses did not match with the clinical responses. Among the 13 patients who achieved pathological complete response (grade 3), the 3 patients were clinical complete response, the 8 patients were clinical partial response, and the 2 patients were clinical incomplete response/stable disease. Among the 13 patients who did not achieved pathological complete response (grade 1 and grade 2), the 2 patients were clinical complete response, the 5 patients were clinical partial response, and the 6 patients were clinical incomplete response/stable disease. Serum samples were collected just before the initiation of neoadjuvant therapy and kept frozen and stored at -80°C until the analysis. This study was approved by the ethics committee of the National Cancer Center and Kobe University Graduate School of Medicine (Hyogo, Japan). Written informed consent was obtained from all subjects.

Chemicals and isotopes

D-arabitol [U- $^{13}\text{C}_5$, 98%], betaine [D11, 98%], glycine [$^{13}\text{C}_2$, 99%; ^{15}N , 99%], L-aspartate [2,3,3- D_3 , 98%], L-serine [$^{13}\text{C}_3$, 99%], and L-arginine [$^{13}\text{C}_6$, 99%] were obtained from Cambridge Isotope Laboratories, Inc. (MA, USA). Methanol was purchased from Kanto Chemical Co., Inc. (Tokyo, Japan), and used as the extraction solution. 2-isopropylmalic acid, which was employed as an internal standard for the GC/MS analysis, was acquired from Sigma-Aldrich (St. Louis, USA). Methoxyamine hydrochloride and N-methyl-N-trimethylsilyl-trifluoroacetamide (MSTFA), which were used for the derivatization, were purchased from Sigma-Aldrich and GL Science (Tokyo, Japan). Ultrapure water (H_2O), acetonitrile (LC/MS grade), formic acid (LC/MS grade), acetic acid (LC/MS grade), and ammonium acetate (LC/MS grade) were obtained from Wako Pure Chemical Industries (Osaka, Japan). Tributylamine, which was used as the ion-pair reagent, was acquired from Sigma-Aldrich. 2-bromohypoxanthine and 10-camphorsulfonic acid, which were employed as internal standards for the LC/MS-based hydrophilic metabolite analysis, were purchased from Sigma-Aldrich. Dilauroylphosphatidylcholine (PC12:0/12:0) was obtained from Avanti Polar Lipids (AL, USA), and it was used as an internal standard for the LC/MS-based lipid analysis.

Sample preparation for GC/MS analysis

The extraction of low molecular weight metabolites was performed according to the method described in our previous report²⁵. Briefly, 20 μ L of each serum sample were mixed with 250 μ L of methanol containing 10 μ L of 0.5 mg/ml 2-isopropylmalic acid as an internal standard. The solution was centrifuged at 19,300 \times g for 5 min, and 200 μ L of the supernatant were evaporated using a vacuum concentrator (TOMY SEIKO SpeedVac), before being lyophilized using a freeze dryer. To induce methoximation, 80 μ L of 20 mg/mL methoxamine hydrochloride dissolved in pyridine were added to the lyophilized sample. Then, 40 μ L of MSTFA (for the derivatization) were added to the sample. The mixture was centrifuged at 19,300 \times g for 5 min, and the supernatant was subjected to GC/MS analysis.

GC/MS analysis procedure

According to the method described in a previous report^{25,26}, the GC/MS analysis was performed using a GCMS-TQ8040 GC/MS/MS system (Shimadzu Co.). Each sample was injected with a split ratio of 1:10, and then the separation was performed on a fused silica capillary column (BPX5; length: 30 m, inner diameter: 0.25 mm I.D., film thickness: 0.25 μ m; Agilent Co). The front inlet temperature was 250°C. Helium gas was used as the GC carrier gas, and argon gas was used as

the MS/MS collision gas. The flow rate of helium gas through the column was 39.0 cm/second. The column temperature was held at 80°C for 2 minutes and then raised by 15°C/min to 330°C, before being held there for 3 minutes. The transfer line and ion-source temperatures were 280 °C and 200 °C, respectively. The ionization voltage was 70 eV. The MRM cycle time was set at 5 cycles/second to allow accurate peak area assessment. The detection of metabolites was carried out using the Smart Metabolites Database (Shimadzu Co.), which contains the relevant multiple reaction monitoring (MRM) method file with data regarding the GC analytical conditions, MRM parameters and retention indices employed for the metabolite measurements of 230 metabolites. Peak identification was performed automatically using the GCMSsolution software (Shimadzu Co.), and the results were confirmed manually based on the specific precursor and product ions, and the retention time. In the semi-quantitative analysis, the peak intensity of each metabolite was normalized to that of the internal standard. In the quantitative analysis of the targeted metabolites, each serum sample was processed in the abovementioned solvent containing the corresponding stable isotopes and was analyzed using the same protocol as was employed for the semi-quantitative analysis. The concentrations of the targeted metabolites in each serum sample were calculated based on standard curves derived from the peak area (y-axis; native/isotope) and concentration (x-axis; native/isotope) ratios.

Sample preparation for the LC/MS-based hydrophilic metabolite analysis

The sample preparation for the LC/MS-based hydrophilic metabolite analysis was performed according to the method described in our previous report²³. Briefly, 20 μ L of each serum sample were mixed with 900 μ L of a solvent mixture (MeOH:H₂O:CHCl₃=2.5:1:1) containing 1 μ M 10-camphorsulfonic acid and 1 μ M 2-bromohypoxanthine as internal standards. The solution was subsequently shaken at 1,400 rpm for 30 min at 37°C, before being centrifuged at 16,000 \times g for 3 min at 4°C. Then, 630 μ L of the supernatant were mixed with 280 μ L of distilled water. The solution was centrifuged at 16,000 \times g for 5 min at 4°C, and 500 μ L of the supernatant were passed through an ultrafiltration filter (Amicon Ultra 0.5 mL centrifugal filters, Ultracel-3K; Merck Millipore, Germany) and then centrifuged at 14,000 \times g for 60 min at 4°C. The collected solution was evaporated using a vacuum concentrator, before being lyophilized using a freeze dryer. The lyophilized sample was reconstituted with 100 μ L distilled water, and the resultant solution was subjected to LC/MS analysis.

LC/MS-based hydrophilic metabolite analysis procedure

According to the method described in a previous report^{23,27}, the LC/MS analysis was

performed using a Nexera LC system (Shimadzu Co.), which was equipped with two LC-30AD pumps, a DGU-20As degasser, an SIL-30AC autosampler, a CTO-20AC column oven, and a CBM-20A control module and coupled with an LCMS-8040 triple quadrupole mass spectrometer (Shimadzu Co.).

The cationic metabolites were separated with a pentafluorophenylpropyl column (Discovery HS F5, 150 mm x 2.1 mm I.D., 3 μ m; SUPELCO, PA, USA) and a guard column (20 mm x 2.1 mm I.D., 3 μ m). The mobile phase for the cationic metabolites consisted of solvent A (0.1% formic acid in water) and solvent B (acetonitrile). The flow rate was 0.3 mL/min, and the column oven temperature was 40°C. The gradient program for mobile phase B was as follows: 0 min, 0%; 7 min, 0%; 20 min, 40%; 20.1 min, 100%; 25 min, 100%; 25.1 min, 0% and 35 min, 0%. The anionic metabolites were separated with an octadecylsilylated silica column (InertSustain C18, 150 mm x 2.1 mm I.D., 3 μ m; GL Sciences, Tokyo, Japan). The mobile phase for the anionic metabolites consisted of solvent A (water containing 15 mM acetic acid and 10 mM tributylamine) and solvent B (methanol). The flow rate was 0.3 mL/min, and the column oven temperature was 35°C. The gradient program for mobile phase B was as follows: 0 min, 0%; 0.5 min, 0%; 20 min, 75%; 20.1 min, 98%; 24 min, 98%; 24.1 min, 0% and 30 min, 0%. To identify hydrophilic metabolites, the m/z value and retention time of each peak were compared with those of authentic chemical standards that had been analyzed using

the same analytical methods. Same as GC/MS procedure, the detection of metabolites was carried out using the database, which contains data on the 123 metabolites for the LC/MS-based cationic metabolites analytical conditions and the 162 metabolites for the LC/MS-based anionic metabolites analytical conditions. In the semi-quantitative analysis, the peak intensity of each metabolite was normalized to that of the internal standard. In the quantitative analysis of the targeted metabolites, each serum sample was processed in the abovementioned solvent containing the corresponding stable isotope and was analyzed using the same protocol as was employed in the semi-quantitative analysis. The concentrations of the targeted metabolites in each serum sample were calculated in the same way as for the GC/MS procedure.

Sample preparation for the LC/MS-based lipophilic metabolite analysis

The sample preparation for the LC/MS-based lipophilic metabolite analysis was performed as follows: 10 μ L of each serum sample were mixed with 90 μ L of methanol containing 10 μ L of 500 ppb dilauroylphosphatidylcholine (PC 12:0/12:0; Avanti Polar Lipids, AL, USA) dissolved in methanol as an internal standard. The solution was placed on ice for 10 min and then centrifuged at 16,000 \times g for 5 min at 4°C. The resultant supernatant was subjected to LC/MS analysis.

LC/MS-based lipophilic metabolite analysis procedure

Lipophilic metabolites were separated using an octadecylsilylated silica column (InertSustain C18, 100 mm x 2.1 mm I.D., 3 μ m; GL Sciences, Tokyo, Japan) and a guard column (10 mm x 3 mm I.D., 5 μ m). The mobile phase for lipids consisted of solvent A (20 mM ammonium acetate in water) and solvent B (methanol). The flow rate was 0.4 mL/min, and the column oven temperature was 40°C. The gradient program for mobile phase B was as follows: 0 min, 80%; 13 min, 98%; 30 min, 98%; 30.1 min, 80% and 35 min, 80%. The putative identification of each peak was conducted based on m/z value and retention time data from an in-house library, because appropriate chemical reference standards could not be obtained. Same as GC/MS procedure, the detection of metabolites was carried out using the database, which contains data on the 285 metabolites for the LC/MS-based lipophilic metabolites analytical conditions.

Statistical analyses

The statistical significance of differences was evaluated using Fisher's exact probability test, the Student's t-test, or the Mann-Whitney U-test. The Mann-Whitney U test was used for non-

normal distribution data and the Student's t-test was used for normal distribution data. Orthogonal partial least squares discriminant analysis (OPLS-DA) was used to understand global metabolic changes between pathological complete response (pCR) group and non-pCR group, and the corresponding variable importance in the projection (VIP) values were calculated in the OPLS-DA model. The area under the receiver operating characteristic (ROC) curve (AUC) was used to assess the feasibility of using the serum levels of particular metabolites as predictive biomarkers. The optimal cut-off values for the selected serum metabolites were determined from their ROC curves. Prognostic factors for the time to progression (TTP) were analyzed using Cox proportional hazards regression analysis. Differences associated with p-values of <0.05 were considered to be statistically significant. After stratifying the patients according to their serum levels of L-serine, time-to-event data were estimated using the Kaplan-Meier method, and the comparisons were made with the log-rank test. The threshold values were the cut-off value calculated using ROC analysis that was evaluated the prediction accuracy of the presence/absence of a pCR response and the values calculated using k-means clustering. OPLS-DA was performed using SIMCA-P+ 12.0 (Umetrics AB, Sweden). Kaplan-Meier curves were created using the R library "survival", and the log-rank test was performed using the statistical software R. All other analyses were carried out using the default conditions of JMP11

(SAS Institute, Inc.).

Results

Patients and treatment outcomes

All 26 patients were able to complete the same neoadjuvant chemoradiotherapy regimen (CDDP plus 5-FU and concurrent radiotherapy) and underwent radical esophagectomy combined with D2 lymphadenectomy. According to previous reports of an association of the prognosis and pCR to neoadjuvant therapy in esophageal cancer patients⁸⁻¹⁰, we divided the patients into two groups based on the pathological responses. Pathological examinations of the surgical specimens revealed that 13 patients achieved pCR (the pCR group, grade 3), while the remaining 13 patients did not achieve pCR (the non-pCR group, grades 1 and 2). No cases were classified as grade 0. The clinical characteristics of the patients are shown in Table 1. There were no significant differences in age, gender, tumor location, or clinical stage between the pCR and non-pCR groups.

Serum metabolites associated with the response of ESCC to chemoradiotherapy

A total of 322 metabolites were detected in the serum samples obtained from the subjects

using untargeted metabolomics analysis. First, the levels of serum metabolites were compared between the pCR and non-pCR groups using the Mann-Whitney U test or Student's t-test. We found that the serum levels of 19 metabolites were significantly lower in the pCR group than in the non-pCR group in the semi-quantitative analysis using the matched internal standards (Table 2). Among the 19 metabolites, 3 (arabitol, uracil, and 3-aminoglutaric acid) were detected by GC/MS analysis, 5 (betaine, glycine, L-aspartate, L-serine, and L-arginine) were detected by the LC/MS-based cation analysis, 1 (2-hydroxyglutaric acid) was detected by LC/MS-based anion analysis, and the remaining 10 metabolites were detected during the LC/MS-based lipid analysis. The volcano plot of the detected lipid species showed a tendency towards the downregulation of phosphatidylethanolamine (PE) production in the pCR group (Fig. 1). The levels of lysophosphatidylethanolamines (LPE) and lysophosphatidylcholines (LPC) also tended to be reduced in the pCR group, although the intergroup differences in the levels of these metabolites were not significant. The OPLS-DA model was constructed to identify the key metabolites that made large contributions to the metabolic profile of pCR group and non-pCR group. The score scatter plots for the LC-MS based lipid species data did not show clear discrimination between the pCR group and non-pCR group (data not shown). The volcano plot of lipid species showed the tendency towards the downregulation of some subclasses of lipids,

but the possibility of the level of single lipid species to be the biomarker candidates for predicting the response to chemoradiotherapy were indistinct (Fig. 1). Next, we performed OPLS-DA for the untargeted metabolomics data except for lipid species. The score scatter plots showed discrimination between the pCR group and non pCR group (Supplemental fig.1). The corresponding S-plot is shown in Supplemental fig. 1. The 16 metabolites of which VIP values obtained from OPLS-DA model were greater than 1.5 were found (Supplemental table 1), and the names of these 16 metabolites were labeled in Supplemental fig. 1.

Quantitative measurements of the serum levels of the predictive biomarker candidates

In the untargeted metabolomics analysis, the serum levels of 19 metabolites exhibited the significant differences between the pCR group and non-pCR group. To obtain more precise quantitative data, we performed a targeted metabolomics analysis in which we used the corresponding stable isotopes. The use of stable isotopes to normalize the serum metabolite concentration data (via internal standardization) made it possible quantify the levels of the targeted metabolites more accurately²⁸. Of the 19 metabolites, we quantitatively analyzed the levels of 6 metabolites including a sugar alcohol (arabitol) and 5 amino acids (betaine, glycine, L-aspartate, L-serine, and L-arginine),

for which we were able to obtain the corresponding stable isotopes. Of the 6 metabolites, VIP values of the 5 metabolites except for arabinol were greater than 1.5 in OPLS-DA. The quantitative evaluations of the serum arabinol level were performed using GC/MS, whereas the analyses of the serum levels of betaine, glycine, L-aspartate, L-serine, and L-arginine were conducted using LC/MS-based cation analysis. Box charts of the serum levels of these 6 metabolites in the pCR and non-pCR groups are shown in Supplemental fig. 2. Based on the quantitative measurements, the levels of serum metabolites were compared between the pCR and non-pCR groups using the Mann-Whitney U test or Student's t-test. We found that the serum levels of 4 metabolites; i.e., arabinol, glycine, L-serine, and L-arginine, were significantly decreased in the pCR group ($p=0.0086$, 0.0345 , 0.0106 , and 0.0373 , respectively). In this study, the 8 patients were stageIIA/IIB, and the 18 patients were stageIIIA/IIIB. There were no significant differences in the serum levels of arabinol, glycine, L-serine, and L-arginine between the stageIIA/IIB patients and stageIIIA/IIIB patients ($p=0.644$, 0.605 , 0.102 , and 0.605 , respectively). The serum levels of betaine and L-aspartate also tended to be decreased in the pCR group ($p=0.0613$ and 0.0734 , respectively) (Table 3a). To evaluate the utility (the predictive accuracy) of the serum concentration of each metabolite for predicting the presence/absence of a pCR response, AUC, sensitivity, and specificity values were calculated using ROC analysis. The optimal serum level

cut-off value for each metabolite was obtained based on the Youden index. As a result, it was found that arabitol, glycine, L-serine, and L-arginine exhibited AUC values of >0.7 for predicting the presence/absence of a pCR response (Table 3b).

Analysis of the prognostic value of the serum metabolites

We evaluated the follow-up information of all patients. At the end of the follow-up period, 16 patients were alive, and 10 patients had died. Among the surviving patients, the median duration of the follow-up period was 55.1 months (range: 42-62; interquartile range [IQR]: 52.6-58.7). As 4 of the 10 deaths were unrelated to ESCC, the TTP and cause-specific survival (CSS) were analyzed to assess prognosis. For the TTP, a Cox proportional hazards regression analysis was conducted using the following variables: age; clinical stage; and the serum levels of arabitol, glycine, L-serine, and L-arginine (i.e., the serum metabolite level cut-off values obtained from the ROC analysis). A previous report showed that the outcome of the patients who achieved pCR with neoadjuvant chemoradiotherapy was favorable compared with that of the patients who did not achieved pCR¹⁰. Therefore, we evaluated the 4 metabolites that were significantly different between the non-pCR group and pCR group. Univariate analysis revealed that only the serum level of L-serine (>110.6 μ M vs.

$\leq 110.6 \mu\text{M}$; hazard ratio, 3.91; $p=0.0463$) was significantly associated with the TTP (Table 4). The Kaplan-Meier method was used to estimate the TTP and CSS. The median TTP and CSS of the patients with higher serum levels of L-serine ($n=11$) was 25.2 months (95% CI 6.3-NA (NA means 'not estimable'.)) and 39.7 months (95% CI 7.6-NA), respectively, and those of the patients with lower serum levels of L-serine were not reached (95% CI 41.1-NA for TTP; NA-NA for CSS). The patients with higher serum levels of L-serine ($n=15$) had inferior prognoses compared with the patients with lower serum levels of L-serine ($p=0.0392$ and $p=0.0204$, respectively, by log-rank test) (Fig. 2a). These tendencies were consistent with the findings of the tertile analysis (Fig. 2b).

Discussion

Cancer cells need to accumulate the “building blocks” of new cellular components, including proteins, lipids, and nucleic acids, and to maintain their cellular redox status, and their attempts to satisfy these requirements result in metabolic alterations. Thus, the metabolic alterations seen in cancer cells have emerged as one of the hallmarks of cancer. There have been several reports for the diagnosis of ESCC using blood-based metabolomics approaches²⁹⁻³². In the previous reports^{31,32}, plasma free amino acid profiles in the ESCC patients were significantly different from those of healthy

people. These results suggest that the increased demand for amino acids to supply the growing tumor is reflected. Therefore, the application of serum samples in order to acquire the overview of the disease or metabolic status of ESCC is considered to be appropriate. There has been a previous report which showed the possibility of the metabolomics approach for predicting the chemoradiosensitivity of ESCC³³. In this report, the plasma levels of 3 metabolites; i.e., LPC(16:1), octanoylcarnitine and decanoylcarnitine, were decreased in the ESCC patients and gradually recovered to the levels of the control group in the responder group. Thus, these 3 metabolites were considered to be the biomarkers for monitoring therapeutic responses of ESCC.

In this study, the 19 metabolites whose serum levels demonstrated significant differences between the pCR group and non-pCR group using untargeted metabolomics analysis were considered to be predictive biomarker candidates. Among the 19 metabolites, several metabolites were reported to have relevant to cancer metabolites. Recently, the importance of one-carbon metabolism to cancer cells has been highlighted³⁴⁻³⁶. One-carbon metabolism is a complex metabolite network involving the folate and methionine cycles. This pathway integrates nutritional components from amino acids, glucose, and vitamins, and it generates various molecules that are important for rapid cancer cell proliferation, including nucleotides; amino acids; and glutathione (GSH) and S-adenosylmethionine,

which are crucial for the maintenance of cellular redox status. Among the metabolites whose serum levels differed significantly between the pCR and non-pCR groups in this study, serine, glycine, and betaine are potential donors of one-carbon units to the folate cycle through one-carbon metabolism. Serine is the third most consumed nutrients after glucose and glutamine³⁷. A recent study showed that rapidly proliferating cancer cells depend on exogenous serine, and serine deprivation reduced the viability and impaired the proliferation of some cancer cells *in vitro* and *in vivo*³⁸. Glycine is an integral component of GSH and purines and is required for cellular proliferation and maintaining the cellular redox balance. Furthermore, glycine is used to provide one-carbon units through the activity of the glycine cleavage system and to produce serine. A recent study detected a correlation between the glycine consumption and proliferation rates of cancer cells³⁹. Arginine is a multi-functional amino acid and is crucial for protein modification; immunoregulation; and the synthesis of several metabolites, such as nitric oxide, urea, ornithine, and citrulline⁴⁰. Several types of cancer involve abnormalities in the primary enzymes involved in arginine metabolism, such as argininosuccinate synthase and depend on extracellular arginine to support their biological processes⁴¹. Recently, the clinical use of arginine deprivation to treat several types of cancer, such as hepatocellular carcinoma, malignant melanoma, prostate cancer, and lymphoblastic leukemia, has been examined, and it was found to be feasible and

effective⁴². Aspartate, which is made from glutamic acid, is a non-essential amino acid and plays important roles in the urea cycle and DNA metabolism. A number of studies have shown that metabolic alterations aimed at maintaining aspartate accumulation support tumor growth^{43,44}. Serine, glycine, betaine, arginine, and aspartate are considered to be required for cancer cell proliferation. Therefore, lower serum concentrations of these metabolites might be unfavorable for cancer cell growth and survival. In this study, the serum concentrations of these metabolites tended to be lower in the pCR group than in the non-pCR group. The lower serum levels of these metabolites may be associated with the tumor malignancy. Arabitol is a polyol, which are sugar alcohols linked to the pentose phosphate pathway. Arabitol was reported to be a candidate serum biomarker of ovarian cancer⁴⁵, but the pathophysiological roles of arabitol are poorly understood, and there were few previous reports about the relation between arabitol and cancer. Therefore, clarifying the functions of arabitol in cancer cells is the subject as the future study. In the untargeted metabolomics analysis conducted in the present study, the serum level of 2-hydroxyglutaric acid was lower in the pCR group than in the non-pCR group. 2-hydroxyglutaric acid has been reported to be an “oncometabolite” in several previous studies⁴⁶. We could not find previous reports to showing the relation between 2-hydroxyglutaric acid and esophageal cancer. However, the relation between D-2-hydroxyglutaric acid and distant metastasis

in colorectal cancer was reported⁴⁷. It might be difficult to achieve pCR in patients whose cancer-related metabolic pathways are upregulated. Although the OPLS-DA for the LC-MS-based lipid species data did not show clear discrimination between the pCR group and non-pCR group, the volcano plot showed the tendency towards the downregulation of some subclasses of lipids. The evaluations of the subclasses of lipids may be useful for predicting the response of esophageal cancer to chemoradiotherapy, although the detailed investigations are needed to be performed in the future.

In this study, all 26 ESCC patients received the same neoadjuvant chemoradiotherapy regimen, which consisted of 5-FU, CDDP, and concurrent radiotherapy. 5-FU is one of the most widely used drugs in cancer therapy. This antimetabolite agent inhibits thymidylate synthetase, which converts deoxyuridine monophosphate (dUMP) to deoxythymidine monophosphate (dTMP), thereby blocking the synthesis of thymidine nucleotides. As a result, DNA replication is inhibited. A correlation was detected between the sensitivity of a tumor to 5-FU treatment and its one-carbon metabolism flux⁴⁸. Therefore, lower serum concentrations of metabolites that are related to one-carbon metabolism (serine, glycine, and betaine) might be favorable both for preventing the proliferation of cancer cells and augmenting their sensitivity to treatment. CDDP is another widely used anticancer drug. It binds to cellular DNA and causes platinum-DNA adduct formation, which prevents DNA

replication. GSH plays an important role in the inactivation of CDDP. CDDP can become conjugated to GSH, which increases its solubility, leading to its excretion. In human ovarian cancer cell lines, an increased cellular level of GSH was found to be related to resistance to CDDP⁴⁹. In human bladder cancer cell lines, the depletion of cellular GSH in CDDP-resistant cells enhanced the cytotoxicity of CDDP⁵⁰. Glycine is one of the components of GSH; therefore, a relationship might exist between the serum concentration of glycine and resistance to CDDP. Several previous studies have reported candidate biomarkers of the chemoradiosensitivity of ESCC⁵¹. The expression of nuclear factor erythroid 2-related factor 2 (Nrf2), which is a critical regulator of intracellular antioxidants, in biopsy specimens obtained before chemoradiotherapy was shown to be correlated with an unfavorable response to neoadjuvant chemoradiotherapy⁵². In addition, Nrf2 gene mutations were demonstrated to be associated with resistance to treatment for advanced ESCC, resulting in worse outcomes, and the downregulation of the expression of the mutated Nrf2 increased the sensitivity of ESCC cells to 5-FU and radiation⁵³. Nrf2 induces the expression of the key serine/glycine biosynthesis enzyme genes PHGDH, PSAT1, and SHMT2 (which encode phosphoglycerate dehydrogenase, phosphoserine aminotransferase 1, and serine hydroxymethyltransferase 2, respectively) to support GSH and nucleotide production in non-small cell lung cancer⁵⁴. Moreover, the expression of murine double

minute 2 (MDM2), which is a key negative regulator of the tumor suppressor protein p53, in biopsy specimens obtained before chemoradiotherapy was found to be a potent predictive marker of chemoradioresistance in advanced ESCC⁵⁵. MDM2 promotes the expression of the serine synthesis pathway enzymes in the presence of serine deprivation⁵⁶. The differences in the serum concentrations of serine and glycine observed between the pCR and non-pCR groups might be explained by these gene mutations.

Conclusion

We found that the pCR group exhibited significantly lower serum concentrations of L-serine, glycine, L-arginine, and arabitol than the non-pCR group. Moreover, it was demonstrated that the serum concentration of serine had the possibility of predicting the prognosis of ESCC patients who received neoadjuvant chemoradiotherapy. However, the limitation of this study is the small sample size, and a further large-scale prospective study is necessary to validate our findings including the multiple testing, and moreover to evaluate the clinical applicability of its findings.

Summary points

- We performed untargeted metabolomics analysis based on gas chromatography/mass spectrometry (GC/MS) and liquid chromatography/mass spectrometry (LC/MS) of serum samples from esophageal cancer patients who received neoadjuvant chemoradiotherapy followed by surgical resection to identify biomarker candidates for predicting the response of esophageal cancer to chemoradiotherapy.
- There were differences between the metabolic profiles of the patients who achieved pathological complete responses (the pCR group) and those who did not (the non-pCR group).
- The 19 metabolites whose serum levels demonstrated significant differences between the two groups were considered to be predictive biomarker candidates.
- To obtain more accurate quantitative data, we performed a targeted metabolomics analysis of the 6 metabolites for which stable isotopes were available (arabitol, betaine, glycine, L-aspartate, L-serine, and L-arginine).
- Arabitol, glycine, L-serine, and L-arginine exhibited significantly lower serum concentrations in the pCR group compared with non-pCR group.
- Univariate Cox regression analysis of the time to progression revealed that a higher serum L-serine concentration was a significant predictor of unfavorable outcomes (hazard ratio, 3.91;

p=0.0463).

- Kaplan-Meier analysis of the time to progression and cause-specific survival revealed that patients with higher serum L-serine concentrations had worse prognoses.
- This study indicates that serum metabolites related to cancer metabolism, including one-carbon metabolism, are potential predictive biomarkers of the chemoradiosensitivity of ESCC.

Figure legends

Figure 1. Volcano plot of the lipid species

X axis: pCR to non-pCR ratio on a log2 scale; Y axis: $-\log_{10}$ (p-value)

P-values were calculated using the Mann-Whitney U-test. The horizontal dashed red line represents a p-value of 0.05. AC: acylcarnitines, FA: fatty acids, LPC: lysophosphatidylcholines, LPE: lysophosphatidylethanolamines, PC: phosphatidylcholines, PE: phosphatidylethanolamines

Figure 2. Kaplan-Meier curves of patients prepared on the basis of the serum concentration of L-serine

The median follow-up period for the surviving patients was 1,652 days (range: 1,260-1,861; IQR:

1,580-1,762). (a) The 11 patients with serum L-serine levels of higher than 110.6 μM exhibited significantly shorter TTP ($p=0.0392$, log-rank test) and worse CSS ($p=0.0204$, log-rank test) than the remaining 15 patients. (b) Significant differences in the Kaplan-Meier curves of the TTP and CSS were detected between the low and high serum L-serine tertiles ($p=0.0253$ and $p=0.00976$, respectively; log-rank test). The threshold values (91.6 μM and 132 μM , respectively) were calculated using k-means clustering.

Table legends

Table 1. Characteristics of the subjects

[†] Tumor location was classified according to the Union for International Cancer Control TNM cancer staging system (7th edition).

[‡] Clinical stage was classified according to the Union for International Cancer Control TNM cancer staging system (7th edition).

pCR, pathological complete response; Lt, lower thoracic esophagus; Mt, middle thoracic esophagus;

Ut, upper thoracic esophagus.

Table 2. Metabolites whose serum levels exhibited significant differences between the non-pCR and pCR groups

(a) Serum metabolites except for lipids

The serum levels of the metabolites were normalized to the peak intensities of the internal standards.

* Fold-change values were calculated based on the pCR to non-pCR ratio.

** P-values were calculated using the Mann-Whitney U-test (except uracil) or Student's t-test (only uracil was normally distributed).

pCR, pathological complete response; SEM, standard error of the mean.

(b) Serum lipid species

The serum levels of the metabolites were normalized to the peak intensities of the internal standards.

† Multiple metabolites are shown in some rows because we could not evaluate the data for these metabolites separately. Therefore, the presented data represent the total values for these metabolites.

* Fold-change values were calculated based on the pCR to non-pCR ratio.

** P-values were calculated using the Mann-Whitney U-test.

pCR, pathological complete response; SEM, standard error of the mean.

Table 3. Evaluation of targeted metabolites

(a) Quantitative evaluation

Of the biomarker candidate metabolites identified in the untargeted metabolomics analysis, 6 metabolites were subjected to targeted metabolomics analysis using the corresponding stable isotopes.

* Fold-change values were calculated based on the pCR to non-pCR ratio.

** P-values were calculated using the Student's t-test (except arabitol) or Mann-Whitney U-test (only the data for arabitol exhibited a non-normal distribution).

pCR, pathological complete response; SEM, standard error of the mean.

(b) Predictive accuracy of the targeted metabolites

Cut-off values were calculated based on the highest Youden index.

AUC, area under the curve; 95% CI, 95% confidence interval.

Table 4. Univariate Cox proportional hazards regression analysis of clinical factors and serum metabolite concentrations associated with the time to progression

Univariate analysis using the Cox proportional hazards model revealed that the serum L-serine level (>110.6 μ M vs. \leq 110.6 μ M; hazard ratio: 3.91; $p=0.0463$) was significantly correlated with the time to progression.

[†] Clinical stage was classified according to the Union for International Cancer Control TNM cancer

staging system (7th edition).

* P-values were calculated using the likelihood ratio test. HR: hazard ratio, 95% CI: 95% confidence interval

HR, hazard ratio; 95% CI, 95% confidence interval.

Supplemental figure 1. OPLS-DA for the untargeted metabolomics data except for lipid species

(a) OPLS-DA score scatter plots showing the discrimination between pCR group (Red) and non-pCR group (Black). The $t[1]$ axis represents the predictive variation among the groups and the $to[1]$ axis represents the variation orthogonal to the group specific variation. The R_2X value were as follows, $R_2X[1]=0.166172$, $R_2X[X \text{ Side Comp.1}]=0.454285$. The ellipse is a 95% Hotelling's T2 ellipse.

(b) OPLS-DA loading S-plot. The names of metabolites whose variable influence on projection (VIP) values were greater than 1.5 were labeled. The $p[1]$ axis represents the magnitude of each variable. The $p(\text{corr})[1]$ axis represents the reliability of each variable.

Supplemental figure 2. Box plot of the targeted metabolites

The boxes denote interquartile ranges. The mean is represented by the horizontal line inside the box.

The whiskers (the lines extending from each box) describe the spread of the data within the 10th and 90th percentiles. The dots represent data points beyond the 10th and 90th percentiles.

Supplemental table 1. The 16 potential biomarkers derived from OPLS-DA

* Fold-change values were calculated based on the pCR to non-pCR ratio.

** P-values were calculated using the Mann-Whitney U-test.

*** VIP values were obtained from the OPLS-DA model.

pCR, pathological complete response; SEM, standard error of the mean.

References

1. Torre LA, Bray F, Siegel RL, Ferlay J, Lortet-tieulent J, Jemal A. Global Cancer Statistics, 2012. *CA a cancer J Clin.* 65(2), 87-108 (2015).
2. Parry K, Visser E, van Rossum PSN, Mohammad NH, Ruurda JP, van Hillegersberg R. Prognosis and Treatment After Diagnosis of Recurrent Esophageal Carcinoma Following Esophagectomy with Curative Intent. *Ann Surg Oncol.* 22 Suppl 3, 1292-1300 (2015).
3. Kelsen DP, Winter KA, Gunderson LL, et al. Long-term results of RTOG trial 8911 (USA

intergroup 113): A random assignment trial comparison of chemotherapy followed by surgery compared with surgery alone for esophageal cancer. *J Clin Oncol.* 25(24), 3719-3725 (2007).

4. Allum WH, Stenning SP, Bancewicz J, Clark PI, Langley RE. Long-term results of a randomized trial of surgery with or without preoperative chemotherapy in esophageal cancer. *J Clin Oncol.* 27(30), 5062-5067 (2009).

5. van Hagen P, Hulshof MCCM, van Lanschot JJB, et al. Preoperative Chemoradiotherapy for Esophageal or Junctional Cancer. *N Engl J Med.* 366(22), 2074-2084 (2012).

6. Shapiro J, van Lanschot JJB, Hulshof MCCM, et al. Neoadjuvant chemoradiotherapy plus surgery versus surgery alone for oesophageal or junctional cancer (CROSS): Long-term results of a randomised controlled trial. *Lancet Oncol.* 16(9), 1090-1098 (2015).

7. Sjoquist KM, Burmeister BH, Smithers BM, et al. Survival after neoadjuvant chemotherapy or chemoradiotherapy for resectable oesophageal carcinoma: An updated meta-analysis. *Lancet Oncol.* 12(7), 681-692 (2011).

8. Berger AC, Farma J, Scott WJ, et al. Complete response to neoadjuvant chemoradiotherapy in esophageal carcinoma is associated with significantly improved survival. *J Clin Oncol.* 23(19), 4330-4337 (2005).

9. Kim MK, Kim S-B, Ahn JH, et al. Treatment outcome and recursive partitioning analysis-based prognostic factors in patients with esophageal squamous cell carcinoma receiving preoperative chemoradiotherapy. *Int J Radiat Oncol Biol Phys.* 71(3), 725-734 (2008).
10. Donahue JM, Nichols FC, Li Z, et al. Complete pathologic response after neoadjuvant chemoradiotherapy for esophageal cancer is associated with enhanced survival. *Ann Thorac Surg.* 87(2), 392-399 (2009).
11. Hsu PK, Chien LI, Huang CS, et al. Comparison of survival among neoadjuvant chemoradiation responders, non-responders and patients receiving primary resection for locally advanced oesophageal squamous cell carcinoma: Does neoadjuvant chemoradiation benefit all? *Interact Cardiovasc Thorac Surg.* 17(3), 460-466 (2013).
12. Seyfried TN, Flores RE, Poff AM, D'Agostino DP. Cancer as a metabolic disease: Implications for novel therapeutics. *Carcinogenesis.* 35(3), 515-527 (2014).
13. Griffin JL, Shockcor JP. Metabolic profiles of cancer cells. *Nat Rev Cancer.* 4(7), 551-561 (2004).
14. Spratlin JL, Serkova NJ, Eckhardt SG. Clinical applications of metabolomics in oncology: A review. *Clin Cancer Res.* 15(2), 431-440 (2009).

15. Zhang A, Sun H, Wang X. Serum metabolomics as a novel diagnostic approach for disease: A systematic review. *Anal Bioanal Chem.* 404(4), 1239-1245 (2012).
16. Liesenfeld DB, Habermann N, Owen RW, Scalbert A, Ulrich CM. Review of mass spectrometry-based metabolomics in cancer research. *Cancer Epidemiol Biomarkers Prev.* 22(12), 2182-2201 (2013).
17. Wishart D, Mandal R, Stanislaus A, Ramirez-Gaona M. Cancer Metabolomics and the Human Metabolome Database. *Metabolites.* 6(1), 1-10 (2016).
18. Nishiumi S, Shinohara M, Ikeda A, et al. Serum metabolomics as a novel diagnostic approach for pancreatic cancer. *Metabolomics.* 6(4), 518-528 (2010).
19. Ooi M, Nishiumi S, Yoshie T, et al. GC/MS-based profiling of amino acids and TCA cycle-related molecules in ulcerative colitis. *Inflamm Res.* 60(9), 831-840 (2011).
20. Shiomi Y, Nishiumi S, Ooi M, et al. GCMS-based metabolomic study in mice with colitis induced by dextran sulfate sodium. *Inflamm Bowel Dis.* 17(11), 2261-2274 (2011).
21. Nishiumi S, Kobayashi T, Ikeda A, et al. A novel serum metabolomics-based diagnostic approach for colorectal cancer. *PLoS One.* 7(7), 1-10 (2012).
22. Kobayashi T, Nishiumi S, Ikeda A, et al. A novel serum metabolomics-based diagnostic

approach to pancreatic cancer. *Cancer Epidemiol Biomarkers Prev.* 22(4), 571-579 (2013).

23. Sakai A, Suzuki M, Kobayashi T, et al. Pancreatic cancer screening using a multiplatform human serum metabolomics system. *Biomark Med.* 10(6), 577-586 (2016).

* This article described the screening method for pancreatic cancer based on the serum metabolomics analysis using GC/MS and LC/MS. Our study applied same protocol of GC/MS and LC/MS analysis.

24. Kojima T, Hashimoto J, Kato K, et al. Feasibility study of neoadjuvant chemoradiotherapy with cisplatin plus 5-fluorouracil and elective nodal irradiation for stage II/III esophageal squamous cell carcinoma. *J Clin Oncol.* 30 Suppl 4, 130 (2012).

* This study was phase II clinical trial of neoadjuvant chemoradiotherapy for locally advanced esophageal squamous cell carcinoma. Our study was performed as additional study of this study.

25. Hirata Y, Kobayashi T, Nishiumi S, et al. Identification of highly sensitive biomarkers that can aid the early detection of pancreatic cancer using GC/MS/MS-based targeted metabolomics. *Clin Chim Acta.* 468, 98-104 (2017).

* This article described the identification of the biomarkers for early detection of pancreatic cancer based on the targeted metabolomics analysis using GC/MS/MS. Our study applied same protocol of

GC/MS/MS analysis.

26. Nishiumi S, Kobayashi T, Kawana S, et al. Investigations in the possibility of early detection of colorectal cancer by gas chromatography/triple-quadrupole mass spectrometry.

Oncotarget; Adv Online Publ Page 5. (2017).

27. Matsubara A, Izumi Y, Nishiumi S, et al. Supercritical fluid extraction as a preparation method for mass spectrometry of dried blood spots. *J Chromatogr B Anal Technol Biomed Life Sci.* 969, 199-204 (2014).

28. Bueschl C, Krska R, Kluger B, Schuhmacher R. Isotopic labeling-assisted metabolomics using LC-MS. *Anal Bioanal Chem.* 405(1), 27-33 (2013).

29. Wang J, Zhang T, Shen X, et al. Serum metabolomics for early diagnosis of esophageal squamous cell carcinoma by UHPLC-QTOF/MS. *Metabolomics.* 12(7), 116-125 (2016).

30. Jin H, Qiao F, Chen L, Lu C, Xu L, Gao X. Serum metabolomic signatures of lymph node metastasis of esophageal squamous cell carcinoma. *J Proteome Res.* 13(9), 4091-4103 (2014).

31. Hasim A, Ma H, Mantimin B, et al. Revealing the metabonomic variation of EC using ¹H-NMR spectroscopy and its association with the clinicopathological characteristics. *Mol Biol Rep.* 39(9), 8955-8964 (2012).

32. Ma H, Hasim A, Mamtimin B, Kong B, Zhang HP, Sheyhidin I. Plasma free amino acid profiling of esophageal cancer using high-performance liquid chromatography spectroscopy. *World J Gastroenterol.* 20(26), 8653-8659 (2014).

33. Xu J, Chen Y, Zhang R, et al. Global and targeted metabolomics of esophageal squamous cell carcinoma discovers potential diagnostic and therapeutic biomarkers. *Mol Cell Proteomics.* 12(5), 1306-1318 (2013).

* This article suggested the possibility of the metabolomics approach to monitor the therapeutic responses of esophageal squamous cell carcinoma.

34. Yang M, Vousden KH. Serine and one-carbon metabolism in cancer. *Nat Rev Cancer.* 16(10), 650-662 (2016).

35. Locasale JW. Serine, glycine and one-carbon units: cancer metabolism in full circle. *Nat Rev Cancer.* 13(8), 572-583 (2013).

36. Meiser J, Vazquez A. Give it or take it: the flux of one-carbon in cancer cells. *FEBS J.* 283(20), 3695-3704 (2016).

37. Hosios AM, Hecht VC, Danai L V., et al. Amino Acids Rather than Glucose Account for the Majority of Cell Mass in Proliferating Mammalian Cells. *Dev Cell.* 36(5), 540-549 (2016).

38. Maddocks ODK, Berkers CR, Mason SM, et al. Serine starvation induces stress and p53-dependent metabolic remodelling in cancer cells. *Nature*. 493, 542-546(2013).

** In this article, the possibility of therapeutic utility of serine depletion was mentioned.

39. Jain M, Nilsson R, Sharma S, et al. Metabolite Profiling Identifies a Key Role for Glycine in Rapid Cancer Cell Proliferation. *Science* 336, 1040-1044 (2012).

40. Morris SM. Arginine metabolism: boundaries of our knowledge. *J Nutr*. 137(6 Suppl 2), 1602-1609 (2007).

41. Dillon BJ, Prieto VG, Curley SA, et al. Incidence and Distribution of Argininosuccinate Synthetase Deficiency in Human Cancers: A Method for Identifying Cancers Sensitive to Arginine Deprivation. *Cancer*. 100(4), 826-833 (2004).

42. Qiu F, Huang J, Sui M. Targeting arginine metabolism pathway to treat arginine-dependent cancers. *Cancer Lett*. 364(1), 1-7 (2015).

43. Rabinovich S, Adler L, Yizhak K, et al. Diversion of aspartate in ASS1-deficient tumours fosters de novo pyrimidine synthesis. *Nature*. 527, 379-383 (2015).

44. Sullivan LB, Gui DY, Heiden MG Vander. Altered metabolite levels in cancer: implications for tumour biology and cancer therapy. *Nat Rev Cancer*. 16(11), 680-693 (2016).

45. Cheng Y, Li L, Zhu B, et al. Expanded metabolomics approach to profiling endogenous carbohydrates in the serum of ovarian cancer patients. *J Sep Sci.* 39(2), 316-323 (2016).
46. Dang L, White DW, Gross S, et al. Cancer-associated IDH1 mutations produce 2-hydroxyglutarate. *Nature.* 462, 739-744 (2009).
47. Colvin H, Nishida N, Konno M, et al. Oncometabolite D-2-Hydroxyglutarate Directly Induces Epithelial-Mesenchymal Transition and is Associated with Distant Metastasis in Colorectal Cancer. *Sci Rep.* 6 (2016): 36289.
48. Ser Z, Gao X, Johnson C, et al. Targeting One Carbon Metabolism with an Antimetabolite Disrupts Pyrimidine Homeostasis and Induces Nucleotide Overflow. *Cell Rep.* 15(11), 2367-2376 (2016).
- ** In this article, the correlation between one carbon metabolism fluxes and 5-fluorouracil sensitivity was demonstrated. Our results may be in line with the results.
49. Byun SS, Kim SW, Choi H, Lee C, Lee E. Augmentation of cisplatin sensitivity in cisplatin-resistant human bladder cancer cells by modulating glutathione concentrations and glutathione-related enzyme activities. *BJU Int.* 95(7), 1086-1090 (2005).
50. Godwin AK, Meister A, O'Dwyer PJ, Huang CS, Hamilton TC, Anderson ME. High

resistance to cisplatin in human ovarian cancer cell lines is associated with marked increase of glutathione synthesis. *Proc Natl Acad Sci U S A*. 89(7), 3070-3074 (1992).

51. Sato Y, Motoyama S, Saito H, Minamiya Y. Novel candidate biomarkers of chemoradiosensitivity in esophageal squamous cell carcinoma: A systematic review. *Eur Surg Res*. 56, 141-153 (2016).

52. Cho JM, Manandhar S, Lee HR, Park HM, Kwak MK. Role of the Nrf2-antioxidant system in cytotoxicity mediated by anticancer cisplatin: Implication to cancer cell resistance. *Cancer Lett*. 260, 96-108 (2008).

53. Shibata T, Kokubu A, Saito S, et al. NRF2 mutation confers malignant potential and resistance to chemoradiation therapy in advanced esophageal squamous cancer. *Neoplasia*. 13(9), 864-873 (2011).

54. DeNicola GM, Chen P-H, Mullarky E, et al. NRF2 regulates serine biosynthesis in non-small cell lung cancer. *Nat Genet*. 47(12), 1475-1481 (2015).

55. Okamoto H, Fujishima F, Kamei T, et al. Murine double minute 2 predicts response of advanced esophageal squamous cell carcinoma to definitive chemoradiotherapy. *BMC Cancer*. 15(1), 208 -216 (2015).

56. Riscal R, Schrepfer E, Arena G, et al. Chromatin-Bound MDM2 Regulates Serine

Metabolism and Redox Homeostasis Independently of p53. *Mol Cell*. 62(6), 890-902 (2016).

Table 1. Characteristics of the subjects

Variable	Histological response		<i>p</i> -value (Fisher's exact t-test)
	Non-pCR (n=13)	pCR (n=13)	
Age			
<65 years	10	7	0.411
≥65 years	3	6	
Gender			
Male	10	13	0.22
Female	3	0	
Tumor location [†]			
Lt	4	7	0.428
Mt	8	6	
Ut	1	0	
Clinical stage [‡]			
IIA	1	0	0.529
IIB	2	5	
IIIA	6	4	
IIIB	4	4	

[†] Tumor location was classified according to the Union for International Cancer Control TNM cancer staging system (7th edition).

[‡] Clinical stage was classified according to the Union for International Cancer Control TNM cancer staging system (7th edition).

pCR, pathological complete response; Lt, lower thoracic esophagus; Mt, middle thoracic esophagus; Ut, upper thoracic esophagus.

Table 2. Metabolites whose serum levels exhibited significant differences between the non-pCR and pCR groups**(a) Serum metabolites except for lipids**

Metabolites	Subclass	Non-pCR (n=13)		pCR (n=13)		Fold change*	<i>p</i> -value**
		Mean	SEM	Mean	SEM		
Arabitol	Sugar alcohols	0.047	0.024	0.011	0.0009	0.233	0.0066
Betaine	Amino acids	1.645	0.161	1.135	0.067	0.69	0.0103
Glycine	Amino acids	1.231	0.071	0.99	0.054	0.804	0.0103
L-aspartate	Amino acids	1.249	0.111	0.958	0.055	0.767	0.021
L-serine	Amino acids	4.43	0.284	3.509	0.11	0.792	0.024
3-aminoglutaric acid	Amino acids	0.561	0.053	0.396	0.027	0.705	0.0313
L-arginine	Amino acids	5.386	0.409	4.147	0.271	0.77	0.0313
Uracil	Pyrimidines	0.0012	0.0001	0.0009	0.0001	0.726	0.0378
2-hydroxyglutaric acid	Organic acids	0.023	0.002	0.016	0.002	0.726	0.0402

The serum levels of the metabolites were normalized to the peak intensities of the internal standards.

* Fold-change values were calculated based on the pCR to non-pCR ratio.

** P-values were calculated using the Mann-Whitney U-test (except uracil) or Student's t-test (only uracil was normally distributed).

pCR, pathological complete response; SEM, standard error of the mean.

(b) Serum lipid species

Metabolites	Non-pCR (n=13)		pCR (n=13)		Fold change [*]	<i>p</i> -value ^{**}
	Mean	SEM	Mean	SEM		
PE (18:1/20:4)	0.157	0.015	0.102	0.008	0.648	0.0056
PE (18:2/20:4)/PE (18:1/20:5)						
PE (16:0/22:6)/PE (16:1/22:5)/ PE (20:2/18:4) [†]	0.799	0.059	0.569	0.051	0.712	0.0089
PE (16:0/20:4)	0.214	0.025	0.15	0.011	0.7	0.0159
PE (18:1/20:3)/PE (18:2/20:2) [†]	0.031	0.004	0.019	0.003	0.606	0.0159
PE (16:1/18:1)/ PE (16:0/18:2) [†]	0.291	0.033	0.198	0.023	0.68	0.0355
PE (16:0/18:1)	0.232	0.028	0.154	0.015	0.663	0.0355
PE (18:0/20:4)	0.576	0.051	0.434	0.037	0.753	0.0355
PE (18:1/22:6)	0.064	0.006	0.044	0.006	0.686	0.0355
LPC (19:0) (sn-2)	0.052	0.005	0.037	0.006	0.72	0.0402
PC (18:1/22:0)	0.074	0.01	0.047	0.006	0.642	0.0402

The serum levels of the metabolites were normalized to the peak intensities of the internal standards.

[†] Multiple metabolites are shown in some rows because we could not evaluate the data for these metabolites separately. Therefore, the presented data represent the total values for these metabolites.

^{*} Fold-change values were calculated based on the pCR to non-pCR ratio.

^{**} P-values were calculated using the Mann-Whitney U-test.

pCR, pathological complete response; SEM, standard error of the mean.

Table 3. Evaluation of targeted metabolites**(a) Quantitative evaluation**

Metabolites	Non-pCR (n=13)		pCR (n=13)		Fold change*	<i>p</i> -value**
	Mean (μM)	SEM	Mean (μM)	SEM		
Arabitol	13.3	5.86	3.72	0.28	0.28	0.0086
Betaine	62.02	7.08	45.9	3.47	0.74	0.0613
Glycine	360.56	32.04	270.94	21.18	0.75	0.0345
L-aspartate	42.57	3.50	34.05	2.62	0.8	0.0734
L-serine	133.99	12.07	96.96	4.37	0.72	0.0106
L-arginine	139.61	11.59	108.27	7.23	0.78	0.0373

Of the biomarker candidate metabolites identified in the comprehensive metabolomics analysis, 6 metabolites were subjected to targeted metabolomics analysis using the corresponding stable isotopes.

* Fold-change values were calculated based on the pCR to non-pCR ratio.

** P-values were calculated using the Student's t-test (except arabitol) or Mann-Whitney U-test (only the data for arabitol exhibited a non-normal distribution).

pCR, pathological complete response; SEM, standard error of the mean.

(b) Predictive accuracy of the targeted metabolites

Metabolites	AUC (95% CI)	Sensitivity (%)	Specificity (%)	Cut-off value (μ M)
Arabitol	0.799 (0.616-0.981)	100	61.5	5.38
Betaine	0.675 (0.437-0.912)	92.3	61.5	55.36
Glycine	0.722 (0.517-0.927)	84.6	61.5	336.32
L-aspartate	0.692 (0.48-0.905)	84.6	61.5	39.58
L-serine	0.781 (0.57-0.992)	92.3	76.9	110.6
L-arginine	0.71 (0.504-0.917)	92.3	46.2	138.77

Cut-off values were calculated based on the highest Youden index.

AUC, area under the curve; 95% CI, 95% confidence interval.

Table 4. Univariate Cox proportional hazards regression analysis of clinical factors and serum metabolite concentrations associated with the time to progression

Variable	Univariate analysis		
	HR	95% CI	<i>p</i> -value*
Age			
≥65 years/<65 years	0.46	0.096-2.24	0.339
Clinical stage [†]			
IIIA or IIIB/IIA or IIB	5.33	0.97-99.3	0.0551
Arabitol			
>5.384 μM/≤5.384 μM	3.08	0.81-12.5	0.097
Glycine			
>336.3 μM/≤336.3 μM	2.34	0.62-9.52	0.2056
L-serine			
>110.6 μM/≤110.6 μM	3.91	1.02-18.7	0.0463
L-arginine			
>138.8 μM/≤138.8 μM	2.77	0.68-10.5	0.1463

Univariate analysis using the Cox proportional hazards model revealed that the serum L-serine level (>110.6 μM vs. ≤110.6 μM; hazard ratio: 3.91; *p*=0.0463) was significantly correlated with the time to progression.

[†] Clinical stage was classified according to the Union for International Cancer Control TNM cancer staging system (7th edition).

* *P*-values were calculated using the likelihood ratio test. HR: hazard ratio, 95% CI: 95% confidence interval

HR, hazard ratio; 95% CI, 95% confidence interval.

Figure 1.

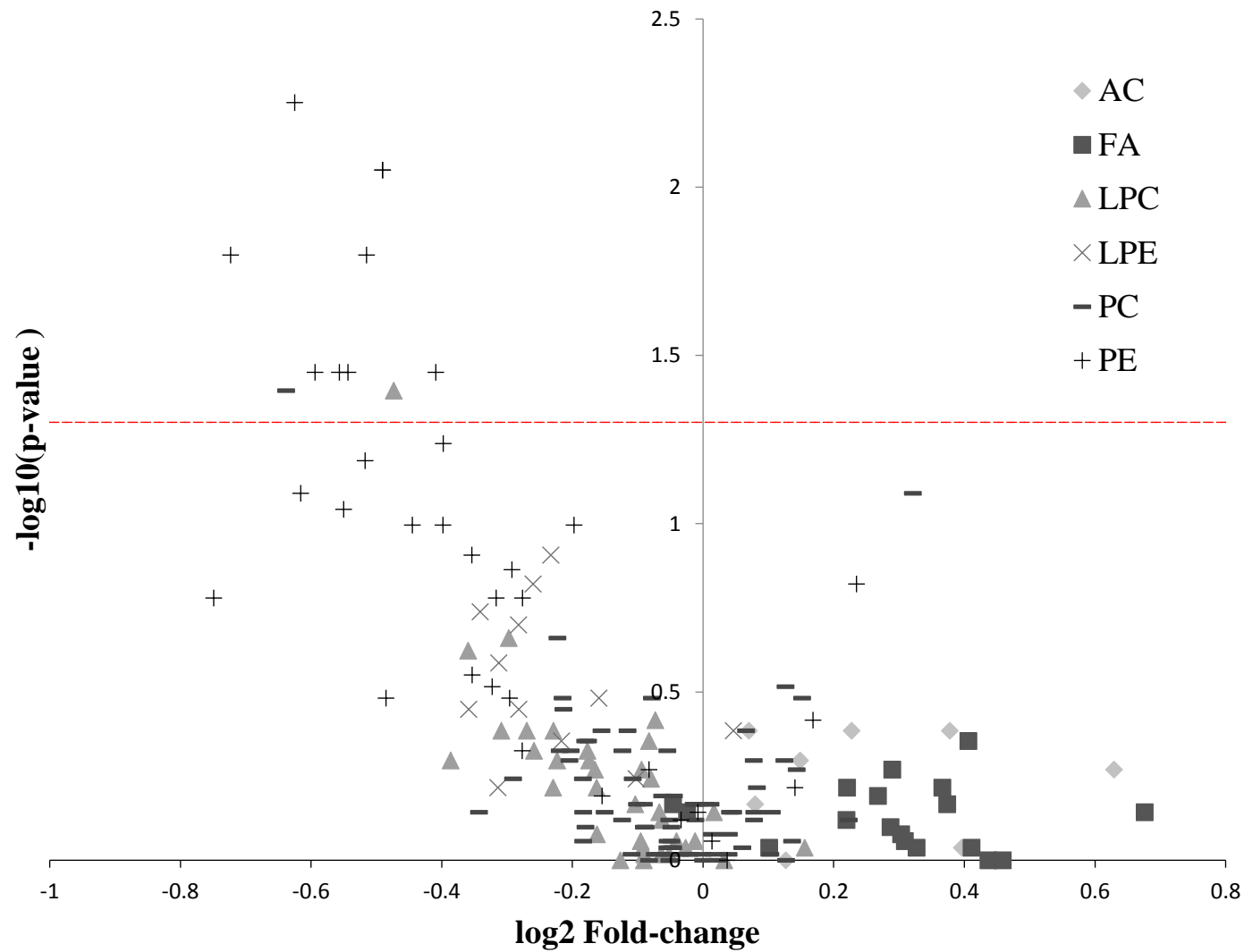
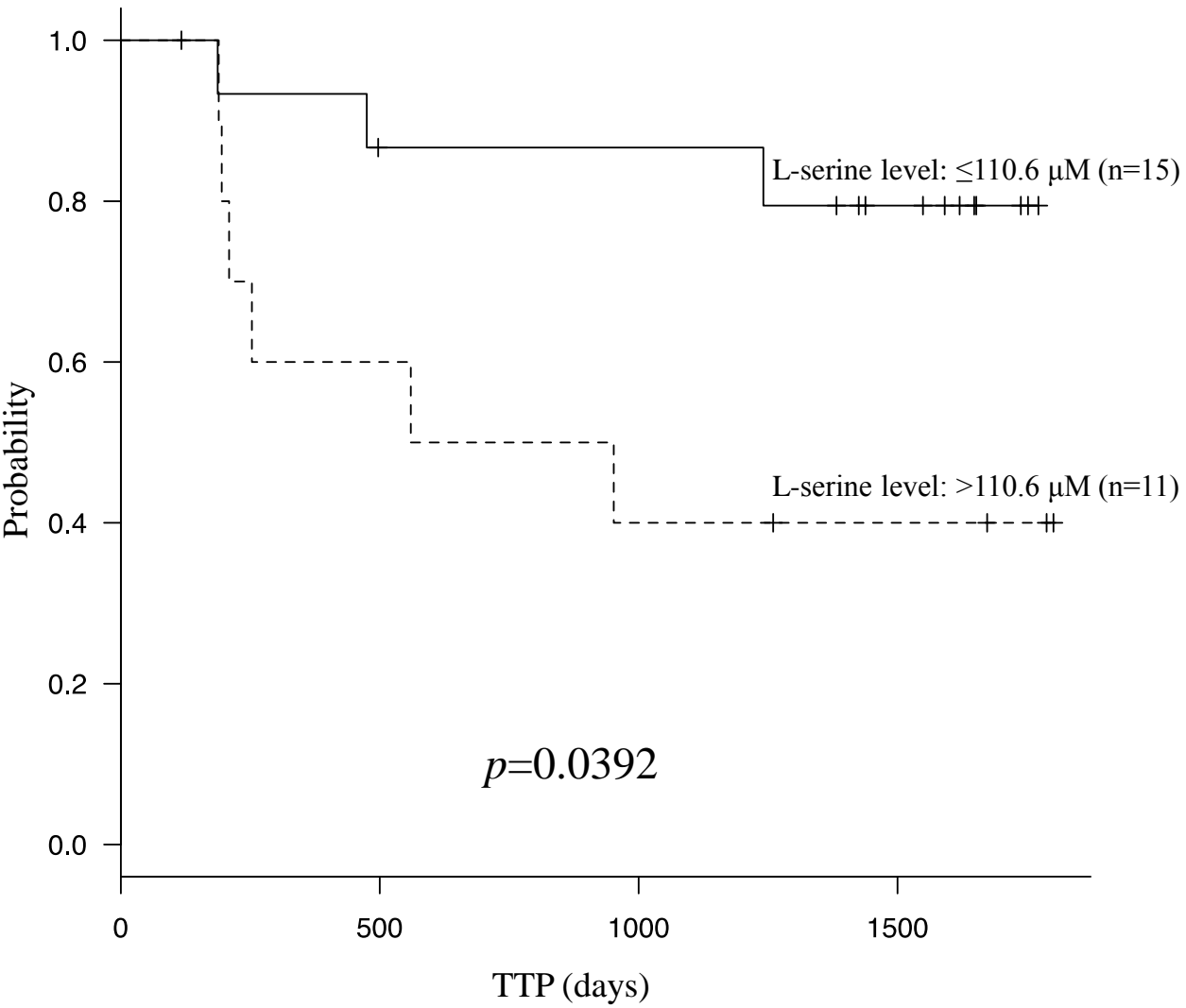


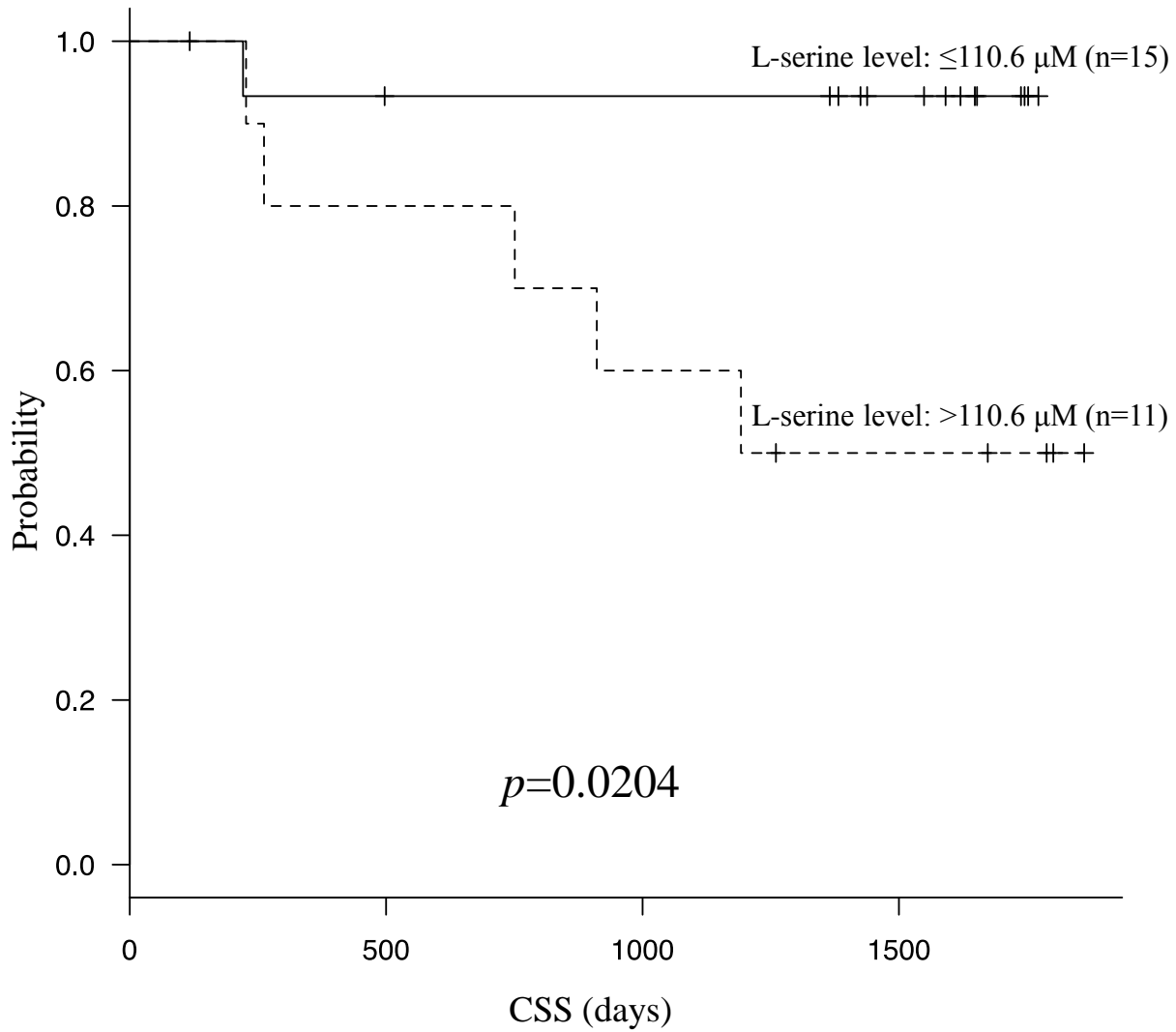
Figure 2.

(a)

Time to progression

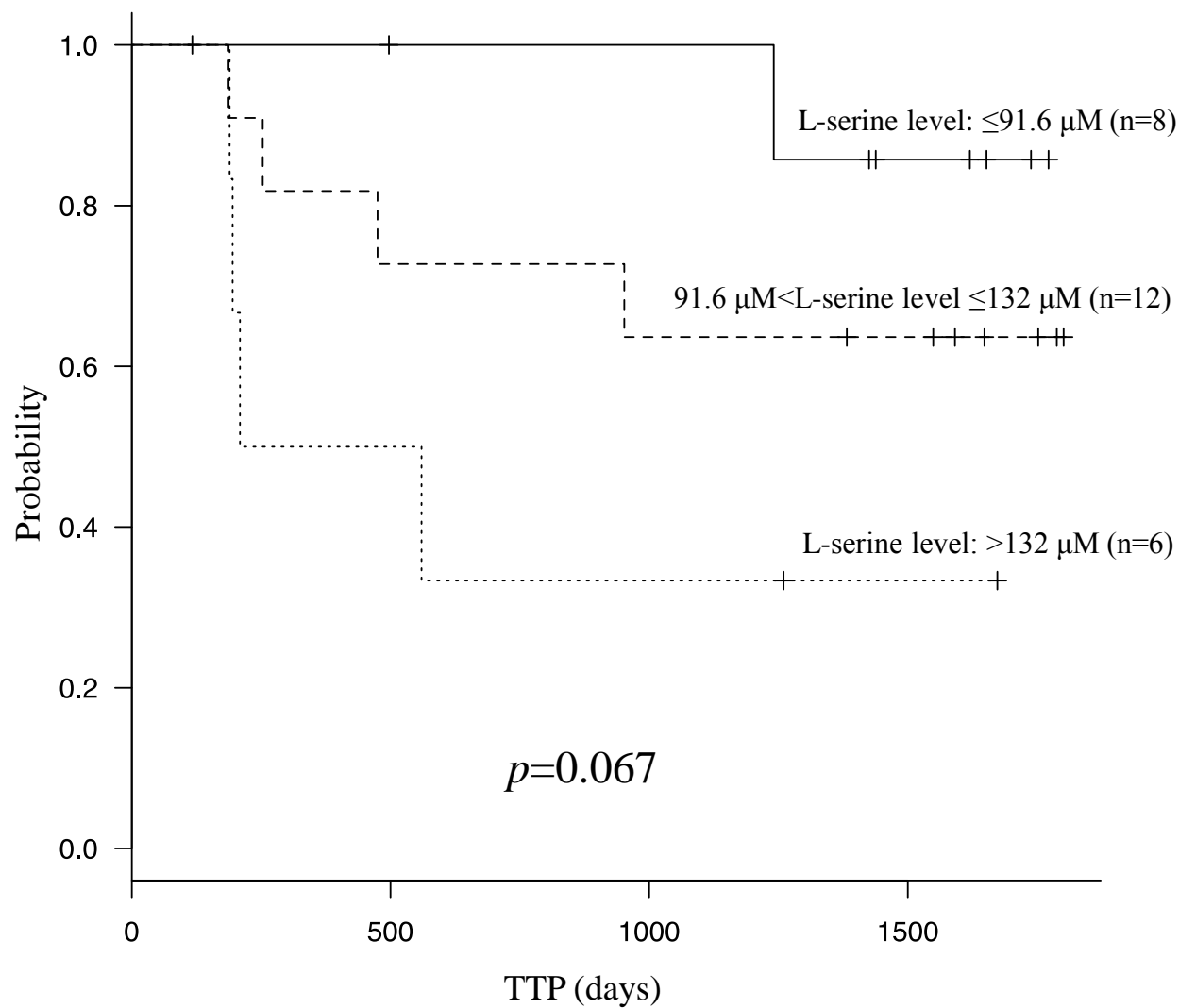


Cause specific survival

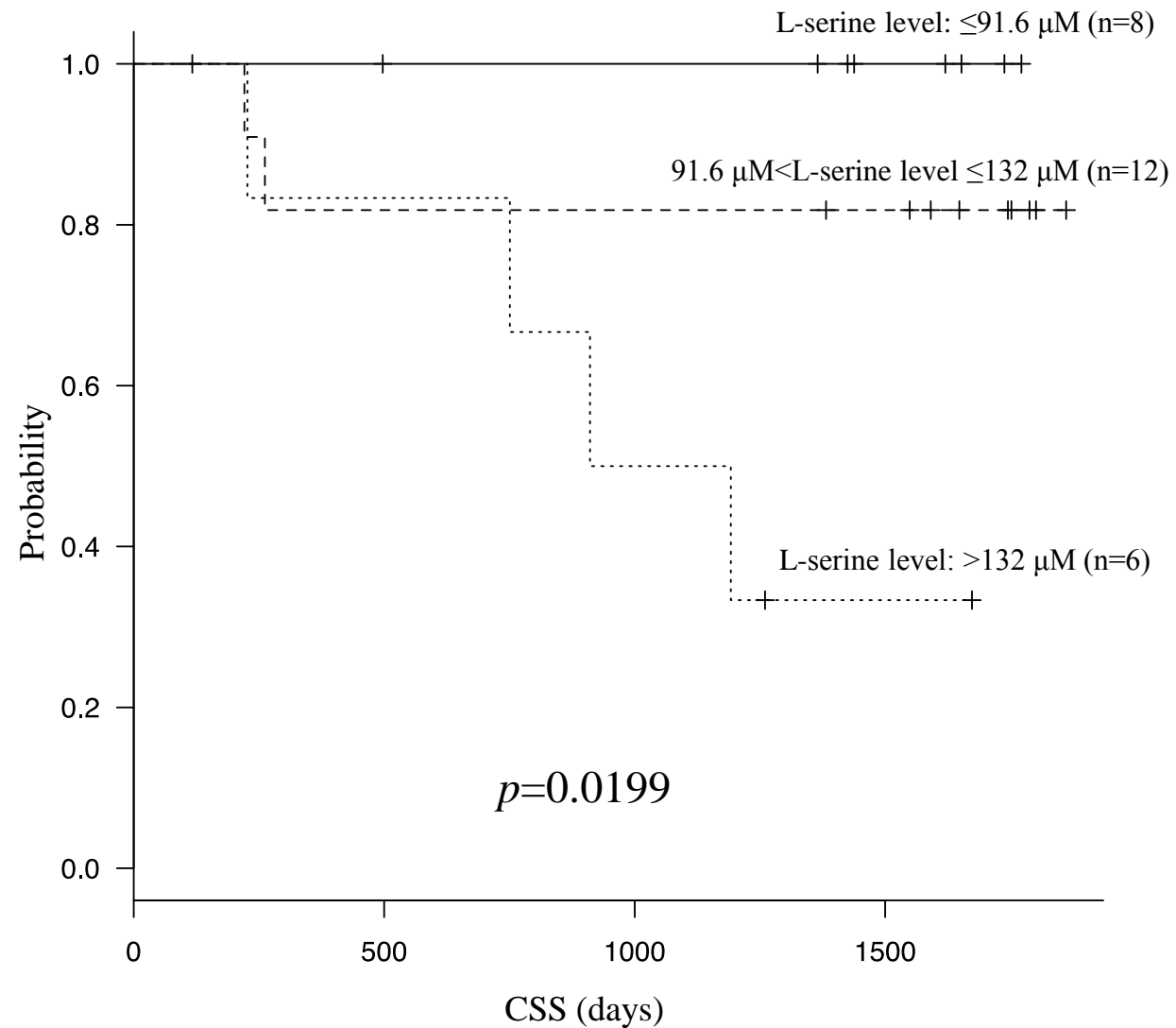


(b)

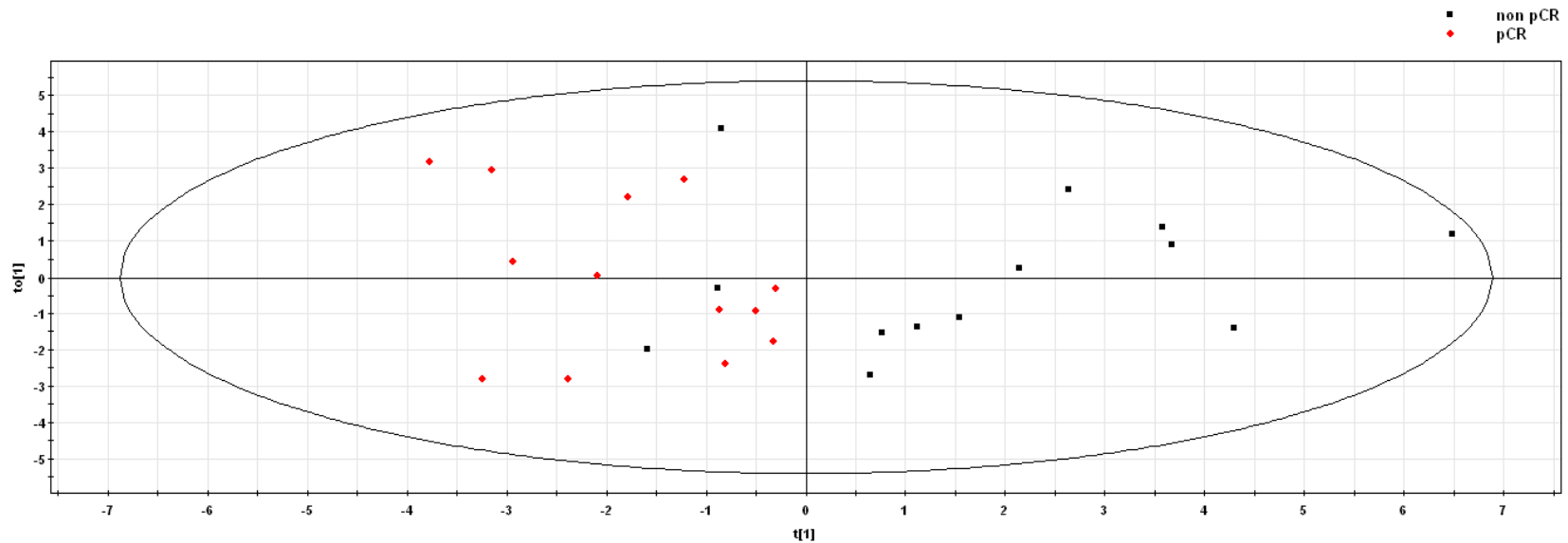
Time to progression



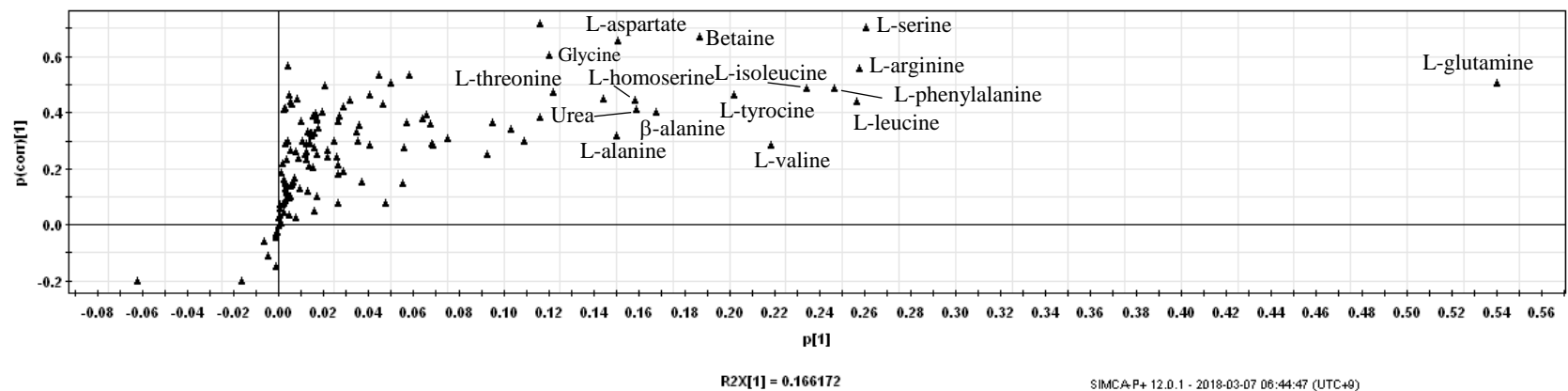
Cause specific survival



(a)

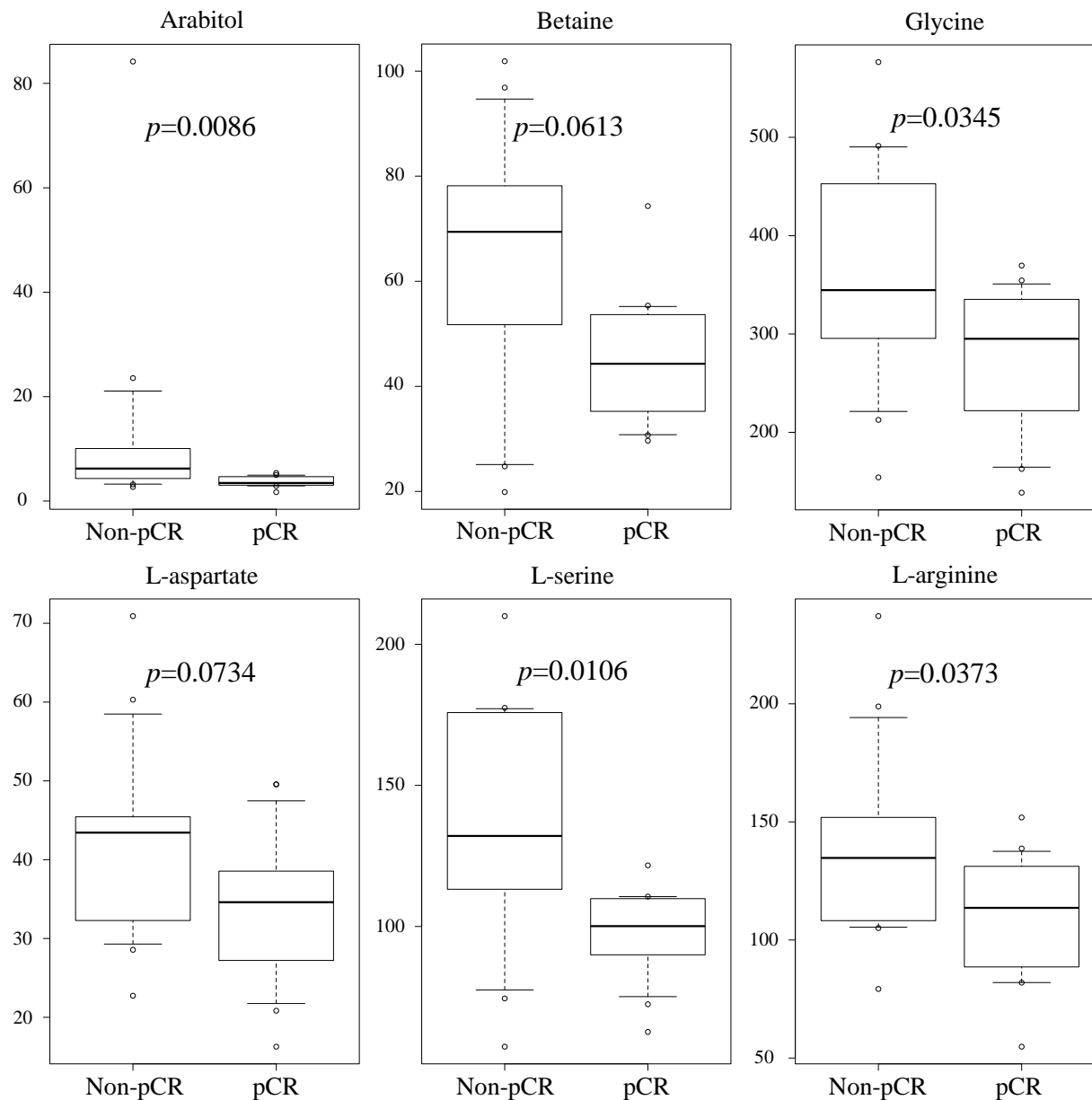


(b)



Supplemental figure 1. OPLS-DA for the untargeted metabolomics data except for lipid species

- (a) OPLS-DA score scatter plots showing the discrimination between pCR group (Red) and non-pCR group (Black). The $t[1]$ axis represents the predictive variation among the groups, and the $to[1]$ axis represents the variation orthogonal to the group specific variation. The R_2X value were as follows, $R_2X[1]=0.166172$, $R_2X[X \text{ Side Comp.1}]=0.454285$. The ellipse is a 95% Hotelling's T2 ellipse.
- (b) OPLS-DA loading S-plot. The names of metabolites whose variable influence on projection (VIP) values were greater than 1.5 were labeled. The $p[1]$ axis represents the magnitude of each variable. The $p(\text{corr})[1]$ axis represents the reliability of each variable.



Supplemental figure 2. Box plot of the targeted metabolites

The boxes denote interquartile ranges. The mean is represented by the horizontal line inside the box. The whiskers (the lines extending from each box) describe the spread of the data within the 10th and 90th percentiles. The dots represent data points beyond the 10th and 90th percentiles.

Supplemental table 1. The 16 potential biomarkers derived from OPLS-DA

Metabolites	Non-pCR (n=13)		pCR (n=13)		Fold change*	<i>p</i> -value**	VIP***
	Mean	SEM	Mean	SEM			
L-glutamine	38.230	1.631	33.811	2.301	0.884	0.1824	5.1245
L-arginine	5.386	0.426	4.147	0.282	0.770	0.0313	3.3356
L-serine	4.430	0.296	3.509	0.115	0.792	0.0240	3.0844
L-leucine	8.081	0.605	6.667	0.583	0.825	0.1370	2.9938
L-phenylalanine	5.786	0.527	4.601	0.334	0.795	0.1119	2.8916
L-valine	14.621	0.995	12.955	1.072	0.886	0.1998	2.7101
L-isoleucine	4.801	0.437	3.770	0.347	0.785	0.1662	2.6637
L-alanine	6.688	0.379	5.762	0.389	0.862	0.1119	2.4382
β-alanine	5.072	0.315	4.274	0.274	0.843	0.1119	2.3798
Betaine	1.645	0.168	1.135	0.070	0.690	0.0103	2.2650
L-tyrosine	2.248	0.216	1.856	0.129	0.826	0.4119	2.2504
Urea	3.551	0.229	2.980	0.287	0.839	0.0812	1.8365
L-homoserine	3.033	0.261	2.578	0.172	0.850	0.2815	1.5908
L-aspartate	1.249	0.116	0.958	0.057	0.767	0.0210	1.5699
L-threonine	2.248	0.216	1.856	0.129	0.826	0.2184	1.5208
Glycine	1.231	0.074	0.990	0.056	0.804	0.0103	1.5088

* Fold-change values were calculated based on the pCR to non-pCR ratio. ** P-values were calculated using the Mann-Whitney U-test.

*** VIP values were obtained from the OPLS-DA model.

pCR, pathological complete response; SEM, standard error of the mean.